

Hydrogen adsorption studies in micro-size cobalt dots

Christian P. Romero · Jonathan I. Avila · Edgardo Cisternas ·
Guerau B. Cabrera · Alejandro L. Cabrera · Kristiaan Temst ·
Margriet J. Van Bael

Received: 30 August 2006 / Accepted: 6 March 2007 / Published online: 3 June 2007
© Springer Science+Business Media, LLC 2007

Abstract Hydrogen desorption curves were obtained from a sample composed of a square arrangement of Co dots with average diameter of 4.4 μm , separated by a distance of 11.6 μm . A macroscopic sample of Co dots grown on a 2.5 \times 2.5 cm Si substrate was made by standard lithographic techniques and used in these experiments. Thermal programmed desorption (TPD) was performed under ultra-high vacuum conditions. Hydrogen TPD curves were obtained from a 1 \times 1 cm Co dots samples displaying a maximum of intensity at 425 K. Hydrogen TPD curve was also obtained from 1 cm \times 1 cm samples of Co films and Co foils for comparison. The hydrogen TPD curves have decreasing intensity from the Co foils to the Co dots and finally to the Co films. This indicates that there are more sites for hydrogen adsorption on the Co dots than in the Co films. This is a surprising result because there is approximately 8.7 times less Co atoms exposed in the Co dots than in the Co film sample. A desorption energy of

27 kcal/mol was obtained for the Co dots suggesting that hydrogen is adsorbed on an hcp hollow site of the Co dot crystalline structure.

Introduction

A research subject of renewed interest in the scientific community is the study of hydrogen gas metals interaction due to the potentially important application it might generate. Nowadays, technological applications of this interaction are found in the chemical industry [1–3] and in hydrogen storage and hydrogen sensors [4, 5] development. Metals or metallic compounds packed in traditional forms such as powders or dispersed metals are used in these applications. In some technological developments, the use of metallic films is appropriate, as in sensors research. On the other hand, due to the intense activity in nanometric-size materials, much progress has been made in the fabrication of samples with reduced shape such as clusters of dots, wires and tubes. At present, it is not well known if these new structures will show any unusual properties regarding the adsorption/absorption of gases, especially in the case of hydrogen. New technological developments in the above-mentioned applications might benefit from the discovery of any unusual properties in these structures. In this work we are studying the adsorption of hydrogen in a square arrangement of Co dots of about 4 μm in diameter. We compared these results with hydrogen desorption from Co film grown on Si substrate and with a Co foil. An attempt to describe the mechanism of hydrogen adsorption or absorption by metals is based on the preferential surface or subsurface sites in the substrate that are occupied by hydrogen, determined by energy minimizing conditions imposed on the system hydrogen/metal [6–8]. By definition,

C. P. Romero · J. I. Avila · E. Cisternas ·
G. B. Cabrera · A. L. Cabrera (✉)
Facultad de Fisica, Pontificia Universidad Catolica de Chile,
V. Mackenna 4860, Macul, Casilla 306 6904411 Santiago 22,
Chile
e-mail: acabrera@uc.cl

K. Temst · M. J. Van Bael
Laboratorium voor Vaste-Stoffysica en Magnetisme,
K.U. Leuven, Celestijnenlaan 200 D, 3001 Leuven, Belgium

Present Address:
C. P. Romero
K.U. Leuven, Celestijnenlaan 200 D, 3001 Leuven, Belgium

Present Address:
G. B. Cabrera
Physics Department, West Virginia University, Hodges Hall,
Box 6315, Morgantown, WV 26506, USA

a subsurface site for hydrogen adsorption would be an interstitial site below the first layer of metal atoms. In fact, Rieder and co-workers [9] defined subsurface site in Pd (111) as an interstitial site between the first and second metal layers. The preferential absorption of hydrogen by these subsurface sites would facilitate hydrogen diffusion into the bulk of the metal.

The system hydrogen/cobalt was well studied in the past [10–12]. Using flat, continuous Co surfaces, it is well accepted that hydrogen remains on the surface after adsorption and dissociation of the adsorbed hydrogen molecule. Insignificant amounts of subsurface hydrogen is found in Co. A significant difference between subsurface adsorption in Pd and other transition metals (Ni, Co, Nb, etc.) was found: Pd easily absorbs large amounts of hydrogen in the bulk (2 hydrogen atoms for every 4 Pd atoms) while the other transition metals do not. The absorption of hydrogen by Pd was tentatively explained (for example [6–8]) using the idea of a process mediated by subsurface bonding of hydrogen. Moreover, transition metals other than Pd, have their surface covered by a native oxide when exposed to air, thus blocking the hydrogen absorption. Hydrogen adsorption by transition metals other than Pd requires cleaning their surface adequately.

Prior to the beginning of these studies we thought that diminishing the Co surface in size (dots of 4 μm in diameter and 38 nm height) would enhance the absorption of hydrogen in subsurface sites. Another possibility was that the study would yield an unexpected result. This was considered plausible since experimental work reporting subsurface adsorption of hydrogen in other metals such as Nb [13] and Cu [14] have also been published. Pick et al. [15, 16] claimed that they were able to activate the Nb surface using a thin overlayer of Pd. According to their results they were successful in detecting large amounts of hydrogen diffusing into the Nb film at 455 K using change of film resistance techniques.

The purpose of our work was to compare the adsorption of hydrogen in samples composed of square arrangements of μm -size Co dots grown on a Si substrate with flat continuous surfaces of Co (foils and films) using Thermal Programmed Desorption (TPD). This comparison consists in: correlating the amount of hydrogen adsorbed with the amount of Co atoms present on the surface and comparing energies of adsorption with crystallographic/morphological information of the Co surface structure obtained by X-ray diffraction (XRD), scanning electron (SEM), transmission electron (TEM) and atomic force (AFM) microscopy.

Understanding the mechanism of hydrogen adsorption/diffusion in metals might lead to understanding why hydrogen easily diffuses inside Pd and not in Co. This is important for developing hydrogen storage devices with less expensive metals than Pd.

Experimental

A sample composed of a square arrangement of Co dots with an average of 4.4 μm in diameter, separated by a distance of 11.6 μm , grown on a 2.5×2.5 cm Si substrate was made by standard lithographic techniques. This sample for the hydrogen desorption experiments was cut into four pieces of 1×1 cm using a diamond knife. The sample was heated using heat transfer from a 304 stainless steel foil (in close contact with the Si substrate) which was resistively heated using a high-current AC power supply.

Several samples of Co film grown on Si substrates were made. A 13 nm thick Co film was grown on several 1×1 cm Si substrates. These substrates were also cut from standard 3 in. diameter, 0.5 mm thick, undoped Si wafer using a diamond knife. The Si wafers were obtained from M.T.I. Corporation. The Co film was grown by physical vapor deposition (PVD) using 99.95% pure Co shots at a pressure of $\sim 10^{-7}$ torr. These samples were also heated using heat transfer from a 304 stainless steel foil (in close contact with the Si substrate) which was resistively heated using the high-current AC power supply.

Samples of pure Co foil with approximate dimensions of $1.0 \times 1.0 \times 0.01$ cm were cut from a larger piece of foil obtained from Alfa Products and mounted on the manipulator. The purity of the foils was 99.999% (Puratronic grade). This sample was resistively heated using a high-current AC power supply.

In order to resistively heat the Co or stainless steel foils using the high-current AC power supply, the following experimental arrangement was made: The foils were spot-welded to two 316 stainless steel wires 0.09 cm in diameter which were clamped on 0.32 cm copper bars of a sample manipulator. The temperature of the foil was monitored by a 0.0127 cm in diameter chromel-alumel thermocouple spot-welded to one face of the foils. When using the samples involving a Si substrate in close contact with the 304 ss, a second chromel-alumel thermocouple was fastened onto the exposed surface of the sample (where the Co dots or film was placed).

Surface analyses

Surface cleanliness and surface elemental composition of the dots, films and foils were monitored with Auger Electron Spectroscopy (AES) in an independent vacuum chamber with a base pressure of 1×10^{-9} torr.

AES analyses were performed with a cylindrical mirror analyzer (CMA) from Staib Instruments, Inc. using 3 keV electrons and 80 nA beam current in pulse counting mode. The spectra were obtained scanning from 100 to 1100 eV energy range. The main surface contaminants were carbon (271 eV) and chlorine (181 eV) for the Co foil. No

chlorine was observed on the Co films. The samples had a thin native cobalt oxide. A treatment was developed to eliminate surface contaminants and the native oxide: the dots, films and foils were subjected to several cycles of flash desorption to 973 K and Ar ion sputtering until a fresh cobalt surface was observed by Auger spectroscopy.

Thermal desorption analyses using the mass spectrometer

The manipulator was placed inside a custom-made vacuum system. The vacuum system mounted on a steel rack consisted in a small—all stainless steel—chamber, a 50 L/s Balzers pump (TPU63) backed with a Leybold Trivac S/D 1.6 B mechanical pump.

A stainless steel 6-way cross was a main part of the vacuum system which allowed us to include: the sample manipulator, an Ar ion sputtering gun, the quadrupole mass spectrometer (Stanford Research System-RGA 200 Gas Analyzer), a Varian variable leak valve and a glass view port. The base pressure of the system after outgassing stayed in the middle 10^{-9} torr. A similar system is described in detail elsewhere [17].

High purity gases (at least 99.999%) from Matheson (AGA Chile) were used in all the experiments described in this work.

X-ray diffraction

X-ray diffraction patterns of the foils and films were taken at room temperature with a Bruker D 8 Advanced Diffractometer, using a copper anode tube ($\lambda_{\text{CuK}\alpha} = 0.154$ nm). The diffraction patterns were obtained with the usual θ - 2θ geometry. The X-ray tube was operated at 40 kV and 40 mA. The goniometer swept between 5° and 140° at $0.02^\circ/\text{s}$ in the whole 2θ interval. The diffracted X-rays were detected with a solid state detector.

Microscopy: optical, atomic force, scanning electron and transmission electron microscopy

We used a Leitz Orthoplan-Pol microscope together with an NPL objective lens (125 \times , 1.3 P). Photographs of the sample with Co dots were obtained with a Leica BDP camera equipped with a Leitz lens (0.32:1).

Atomic force microscopy (AFM) was performed in ambient conditions with a home-made AFM in contact mode, with a n⁺-Si cantilever from Nanosensor ($f_{\text{res}} = 13$ kHz). The scan range of the scanner was calibrated with ULTRASHARP calibration gratings from MicroMasch (TGZ02 and TGX01). The software for image analyses used was SXM, developed at University of Basel, Switzerland. This system is described in detail elsewhere [18].

Scanning electron microscopy (SEM) was performed with a Leo 1400 VP microscope, using 10 keV electrons, 100 μA beam current and a working distance of 6 mm. The microscope was operated at high vacuum ($\sim 10^{-6}$ mbar).

High resolution transmission electron Microscopy (HR-TEM) was performed with an FEI TEM model Tecnai G2 F20 S-Twin equipped with a field emission electron gun able to collimate the electron beam down to a spot of 2 \AA in diameter. The Electron beam can be accelerated from 80 to 200 kV. The microscope includes a CCD camera model GATAN 794 and an EDAX detector for micro-analyses of dispersed X-rays.

Results and discussion

Characterization of Co films and Co foils

The X-ray diffraction pattern of the Co foil corresponds to the usual hexagonal lattice of Co. A preferential orientation of the grains, due to the rolling, in the (101) and (102) direction is observed and remained after annealing the foils up to 900 K. A significant diffraction line in the (002) direction is also observed before annealing. The diffraction pattern of the Co foil showed visible background as a result of fluorescent scattering. Microscopic characterization of surface roughness of the foils was done by AFM. The foils are very rough due to the cold rolling. One can see lines of “mountains” separated by “valleys” on a regular arrangement. The “valleys” are 2 μm wide and the “mountains” 1 μm in high.

The X-ray diffraction pattern of the Co films shows the usual hexagonal pattern. The Co films are strongly c-oriented (002), as seen from grazing incidence XRD patterns. The diffraction patterns did not show any significant background signal. Microscopic characterization of surface roughness of the Co films was done by AFM. The films were so smooth that it was impossible to see any features with the resolution of the AFM.

Microscopic characterization of the Co dots

The Co dots samples were inspected by optical microscopy in order to count the dots missing or misplaced from the square arrangement. The diameter of the dots and the distances between dots were measured. A photograph of an area of the sample with Co dots in which 47 dots appear is displayed in Fig. 1. This is a characteristic photograph of many of the areas inspected. The position in the square arrangement where the dots should be located is labeled with a number. A Co dot corresponding to position 21 is missing (dots in positions 5 and 37 are small but not

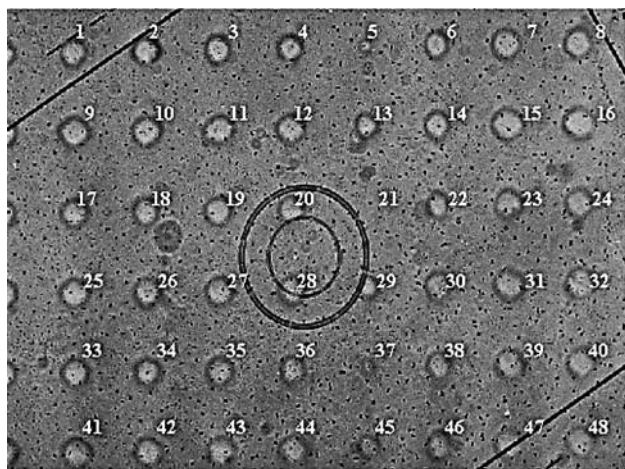


Fig. 1 Photograph of an area of the sample with Co dots in which 47 dots appear. Photograph taken with an optical microscope using magnification 531 \times

missing). The area covered by this photograph is approximately $67.7 \times 94.8 \mu\text{m}$ and contains 47 dots. Therefore, in a typical sample of $10 \times 10 \text{ mm}$ used for the TPD experiments, there are approximately 732,320 dots on the surface of the Si. SEM inspection of the samples was performed in order to measure the size of the dots. A typical SEM image of the samples is displayed in Fig. 2. A red circle was drawn around the biggest and the smallest dot displayed in the picture in order to measure the respective diameters. These diameters were 4.9 and $3.7 \mu\text{m}$ respectively. A statistical study of the diameter of the dots in an area of $2 \times 1 \text{ mm}$ was done using optical microscopy, resulting in $4.4 \mu\text{m}$ the average size. The height of the dots was determined from an AFM profile and the roughness of the dots was determined by statistical processing a AFM surface morphology image of a dot. A typical AFM profile is displayed in Fig. 3. The dots had a 38 nm height and the

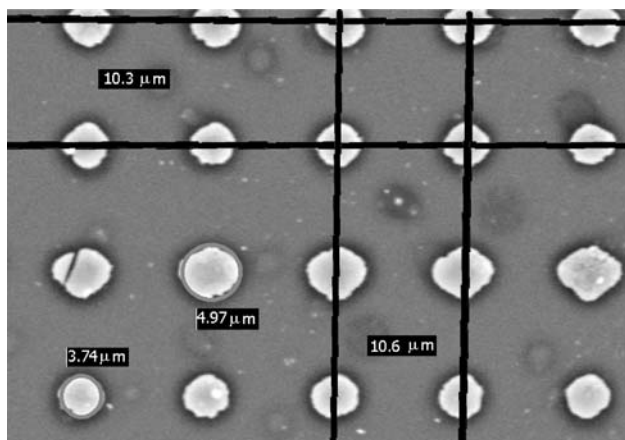


Fig. 2 SEM image of the Co dot sample. Dark lines were drawn to measure the distance between dots. Red circles were drawn to estimate diameter of dots

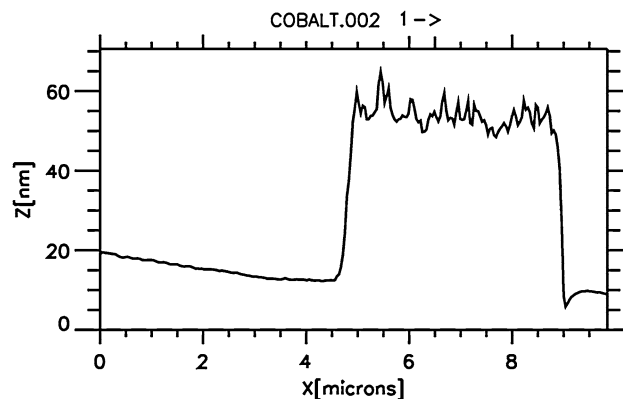


Fig. 3 AFM profile of a single Co dot in a sample of Co dots over Si substrate

roughness resulted in 2.6 nm on average. The geometrical surface area of an average dot exposed to hydrogen was $15.21 \mu\text{m}^2$ for the flat top surface of the dot plus $0.53 \mu\text{m}^2$ for the surface of the exposed edge. This gives a total surface area of $15.74 \mu\text{m}^2$ or $1.57 \times 10^{-7} \text{ cm}^2$. Taking all the dots present in a sample of $1 \times 1 \text{ cm}$ (732,320 dots) the total physical area of Co exposed to hydrogen was $732,320 \times 1.57 \times 10^{-7} \text{ cm}^2$ or 0.115 cm^2 . This is approximately 8.7 times less area than that found in a fresh $1 \times 1 \text{ cm}$ Co film surface. We prepared a piece of the Co dots sample for HR-TEM inspection. A disk of 3 mm in diameter and 0.1 mm in thickness was cut from the sample and mechanically eroded at the center to 10 μm in thickness. The center of the disk was then exposed to ion milling until a hole was made and the edge of the hole was thin enough for TEM inspection. Several dots were found at the edge of the hole. Real images at high magnification revealed that the structure of the approximately 3–4 μm dots observed was polycrystalline. The dots were composed of Co crystals of approximately 20 nm in diameter. After selecting a Co dot, the operation of the TEM was changed to selected area diffraction (SAD) mode and several electron diffraction patterns were obtained. All of them showed bright circles characteristic of the polycrystalline structure. The fitting of the atomic spacing from the size of the diffraction circles yield a hexagonal crystal structure for the Co dots. The lattice constants obtained were $a = 2.46 \text{ \AA}$ and $c = 3.99 \pm 0.2 \text{ \AA}$. A typical diffraction pattern with the Miller indexes of the Co planes corresponding to each diffraction circle is shown in Fig. 4

Hydrogen desorption from Co dots, Co films and Co foils

The Co dot samples, the Co film samples and the Co foils were subjected to several cycles of flash desorption to 973 K in vacuum and Ar ion sputtering with the purpose of

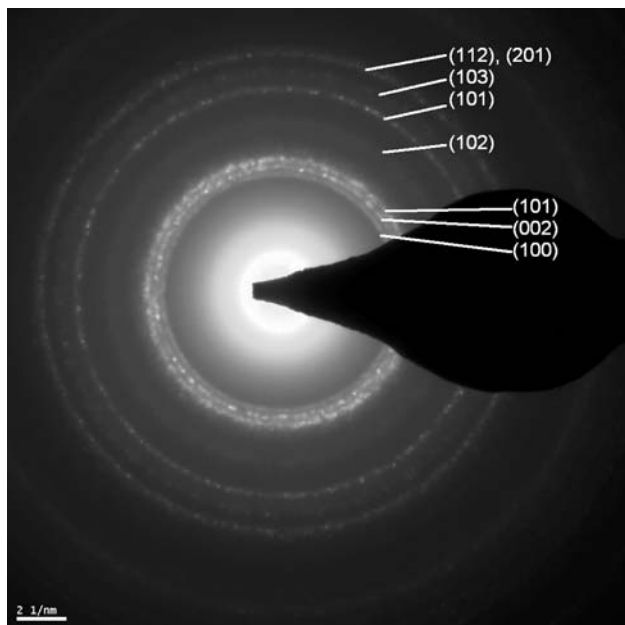


Fig. 4 Selected area diffraction (SAD) from a Co dot. Bright circles are characteristic of a Co polycrystalline structure. Miller indexes of Co planes are included. Lattice constant obtained from this pattern corresponds to a Co hexagonal structure

reducing contamination and surface oxide (without this treatment there was no hydrogen adsorption). Ar ion sputtering on the Co dots and films was performed using more gentle conditions than in the case of a Co foil. Typically, a 500 eV Ar ions were used for 30 s sputtering time.

All the samples were then exposed to 1200 L of H₂ at room temperature in order to perform the desorption experiments (1 L = 10⁻⁶ torr·s).

After the dosing with gas, the Co foils were heated to 973 K, at a rate of 5 K/s, and the desorbing gas was detected with the mass spectrometer. The Co-dots on Si and Co-films on Si were heated to 1070 K at an effective surface rate of 1.5 K/s. The 304 ss foil (the heater) was heated at a rate of 5 K/s but due to slow heat transfer through the Si substrate, the surface of the samples was heated only at 1.5 K/s during the 154 s that data was recorded. Typical spectra of hydrogen desorption from a piece of 1 × 1 cm of Co dots, Co film and a Co foil after exposures to 1200 L are displayed in Fig. 5.

A 1 × 1 cm pure Si substrate was also used as a control in the hydrogen desorption experiments. No hydrogen was desorbed from the pure Si substrate indicating that there was no hydrogen adsorption after dosing the Si with 1200 L of hydrogen.

A broad peak of hydrogen reaching a maximum at about 425 K was detected in the desorption experiment using a Co foil. This curve is similar to another one obtained in prior work on hydrogen desorption from Co foils [19]. We observed that this type of curve can be fitted with two nearly

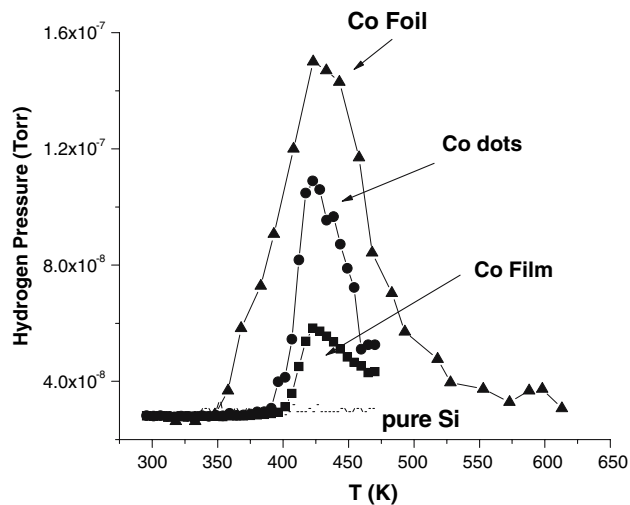


Fig. 5 TPD spectra for H₂ desorption after exposure to 1200: filled triangles—pure Co foils using a heating rate of 5 K/s; filled circles—Co dots using a heating rate of 1.5 K/s; filled squares—Co film using a heating rate of 1.5 K/s; dotted line—pure Si substrate

Gaussian curves which correspond to two desorption peaks associated to the adsorption states β_1 and β_2 , observed in most transition metals. At the high hydrogen dosage that these experiments were performed, the β_1 adsorption state is completely populated and the energy of desorption obtained results independent of dosage and had lower values than other studies with coverages lower than one.

The hydrogen desorption curves from the Co films and Co dots result in a peak reaching a maximum at 425 K. The peaks have decreasing intensity from the Co foils, Co dots and Co films. The area under each curve is proportional to the number of hydrogen atoms adsorbed. This indicates that the Co dots adsorbed more hydrogen than the Co films: a surprising result because there are 8.7 times less Co atoms exposed in the Co dots in comparison with the Co film. The effective area for hydrogen adsorption in the Co foil is twice the size of the Co film, because in the case of the foil two Co faces of 1 × 1 cm are exposed to hydrogen.

Calculation of desorption energies

Activation energy for desorption corresponding to a single peak can be obtained by plotting the rate constant versus the inverse absolute temperature. The kinetic parameters are often coverage dependent [20] but in our work the exposures were constant for the three systems studied.

The rate constant (k) is defined in the rate equation for desorption:

$$dN/dt = -kN^n \tag{1}$$

where dN/dt is the rate of desorption, N is the concentration of adsorbed gas and n is the order of desorption. Since H₂

molecules dissociate on the surface of transition metals, the order n taken as 2 in the analysis is plausible, but the order n is determined by the best fit of the data to a straight line in an Arrhenius plot. The rate constant k normally obeys an Arrhenius-type rate law of the form:

$$k = v_n \exp(-E/RT) \quad (2)$$

where v_n is a pre-exponential factor, R is the gas constant, T the temperature and E is the activation energy.

Redhead [21] derived a simplified equation for second order desorption:

$$E/RT_p^2 = (v_n N/\beta) \exp(E/RT_p) \quad (3)$$

In this case T_p is the temperature corresponding to the maximum of the desorption curve.

A graphic solution for Eq. (3) gives a value of 26 kcal/mol. For E , this was done assuming $v_2 = 10^{13} \text{ s}^{-1}$. Somorjai discusses the vibration values of adsorbed atoms and molecules in his book [20, p. 324] and a value of 10^{13} s^{-1} for the pre-exponential factor seems to be adequate for hydrogen. This frequency of vibration was determined in experiments using high resolution electron loss spectroscopy (HREELS).

Following the same procedure, we calculated the hydrogen desorption energy from the Co film and Co dots assuming $v_2 = 10^{13} \text{ s}^{-1}$. A graphic solution for Eq. (3) gives an energy of 27 kcal/mol.

We did prior studies of hydrogen desorption from Co powders [19] and Co foils [22] and we obtained energy values for the β_1 and β_2 of 22.2 and 28.8 kcal/mol respectively. These experiments were done under similar conditions of full hydrogen coverage. Our work is not focused on obtaining an accurate hydrogen desorption energy from different Co surfaces but only using these energies as a comparison between the mechanism of hydrogen adsorption first on one surface and then on another.

The values that we obtained are not unreasonable compared with 21 kcal/mol obtained on Co (001) single crystal [23] and a recent result of computer simulation work yielded 28 kcal/mol for hydrogen adsorbed on an hcp hollow site on Co (001) [24].

Conclusions

Hydrogen TPD curves were obtained from Co films and Co dots samples which peaked at 425 K. A hydrogen TPD

curve was also obtained from a Co foil as a comparison. The hydrogen TPD curves have decreasing intensity from the Co foils to the Co dots and to the Co films. This indicates that there are more sites for hydrogen adsorption on the Co dots than in the Co films. This is a surprising result because there are approximately 8.7 times less Co atoms exposed in the Co dots that in the Co film. A desorption energy of 27 kcal/mol was obtained for the Co dots suggesting that hydrogen is adsorbed on an hcp or fcc hollow site of the Co dot crystalline structure.

Acknowledgements This research was partially supported by grants from the Chilean Government (FONDECYT 1030642 and 1060634), Fundacion Andes and MECESUP PUC0006 and UCh0205. We thank M. Moreno for SEM analyses, A. Zuñiga for HR-TEM analyses, M. Pino for XRD analyses, J. P. Staforelli and A. Pernas for helping with the TDS experiments and optical characterization of the Co dots.

References

- Gryaznov VM (1986) Vestn Akad Nauk SSSR 21
- Gryaznov VM (1986) Platinum Met Rev 30:68
- Shu J, Grandjean BPA, Van Neste A, Kaliaguine S (1991) Can J Chem Eng 69:1036
- Klose F, Rehm Ch, Nagengast D, Maletta H, Weidinger A (1997) Phys Rev Lett 78:1150
- Rehm Ch, Fritzsche H, Maletta H, Klose F (1999) Phys Rev B 59:3142
- Lagos M (1982) Surf Sci Lett 122:L601
- Lagos M, Schuller IK (1984) Surf Sci 138:L161
- Lagos M, Martinez G, Schuller IK (1985) Phys Rev B 29:5979
- Rieder KH, Baumberger M, Stocker W (1983) Phys Rev Lett 51:1799
- Vannice MA (1975) J Catal 37:449
- Somorjai GA (1981) Catal Rev Sci Eng 23:189
- Cabrera AL (1993) J Vac Sci Technol A 11(1):205
- Li Y, Erskine JL, Diebold AC (1986) Phys Rev B 34:5951
- Rieder KH, Stocker W (1986) Phys Rev Lett 57:2548
- Pick MA, Davenport JW, Strongin M, Dienes GJ (1979) Phys Rev Lett 43:286
- Pick MA (1981) Phys Rev B 24:4287
- Cabrera AL, Morales E, Altamirano L, Espinoza P (1993) Rev Mex Fis 39:932
- Tarrach G, Lagos P, Hermans R (2001) Acta Microsc 10(Supplement 1):185
- Cabrera AL (1993) J Vac Sci Technol A 11:205
- Somorjai GA (1994) Introduction to surface chemistry and catalysis. John Wiley & Sons, Inc., New York, p 313
- Redhead PA (1962) Vacuum 12:203
- Cabrera AL, Espinosa-Gangas J, Jonsson-Akerman J, Schuller IK (2002) J Mater Res 17:2698
- Bridges M, Comrie C, Lambert R (1979) J Catal 58:28
- Klinke DJ II, Broadbelt LJ (1999) Surf Sci 429:169